Density Functional Theory of Realistic Models of Polyethylene Liquids in Slit Pores: Comparison with Monte Carlo Simulations†

Shyamal K. Nath,*,‡ John G. Curro,§,|| and John D. McCoy‡

Department of Materials Engineering, New Mexico Tech, Socorro, New Mexico 87801, Sandia National Laboratories, Albuquerque, New Mexico 87185, and Department of Chemical & Nuclear Engineering, University of New Mexico, Albuquerque, New Mexico 87131

Received: September 28, 2004; In Final Form: November 1, 2004

Density functional theory is applied to study properties of fully detailed, realistic models of polyethylene liquids near surfaces and compared to results from Monte Carlo simulations. When the direct correlation functions from polymer reference interaction site model (PRISM) theory are used as input, the theory somewhat underpredicts the density oscillations near the surface. However, good agreement with simulation is obtained with empirical scaling of the PRISM-predicted direct correlation functions. Effects of attractive interactions are treated using the random-phase approximation. The results of theoretical predictions for the attractive system are also in reasonable agreement with simulation results. In general, the theory performs best when the wall−polymer interaction strength is comparable to polymer−polymer interactions.

I. Introduction

The understanding of the structure of polymers near surfaces is important for a wide range of scientific and technological problems. Examples of such problems are wetting and adhesion, self-assembly of block copolymers near chemically heterogeneous surfaces, and self-assembly of biological molecules. To date, many theoretical and simulation studies have been devoted to understanding of the properties of such systems. Although molecular dynamics (MD) or Monte Carlo (MC) simulations provide a direct, formally exact approach in dealing with atomistically detailed models of polymers, they are often computationally intensive and expensive. By contrast, theoretical approaches are computationally much less demanding but they often require coarse-graining of the models to be tractable. Development of a theoretical approach that is computationally convenient but can still capture all the atomistic details of polymer systems is thus a very attractive goal. The purpose of the present study is to demonstrate that full, atomistically detailed realistic polymer models can be treated within the well-known density functional theory (DFT) approach to study the properties of polymers near surfaces.

Our theoretical approach is based on the class of molecular density functional theory that uses the structure of the homogeneous liquid as input. Structure-based density functional theory was first extended to molecular systems by Chandler, McCoy, and Singer (CMS).[1−3] Sen et al.[4,5] first used this theory in studying properties of polymers near surfaces. They studied a homopolymer tridecane melt near a hard surface. In their study, the intrachain interactions were formulated within the rotational-isomeric-state[6] (RIS) model and the interchain interactions were hard in nature. They showed that almost quantitative agreement with molecular dynamics simulation of a Lennard-Jones (LJ) tridecane could be obtained by adjusting the hard sphere diameter of the methylene group in their model tridecane molecules. To the best of our knowledge, this is the most detailed polymer model that has been studied within the CMS density functional theory until now. Other formulations of DFT that use the equation-of-state of the bulk liquid as input have also been developed.[7−10]

Recently, Frischknecht and Curro[11] performed a detailed study of properties of polymer melts near surfaces using the random-walk version of the CMS density functional theory. The principal idea in the density functional theory is to convert the many-chain system to a system consisting of a single chain in an effective medium-induced field. The structure of the many-chain system is then obtained by performing a Monte Carlo simulation of the single chain in the medium-induced field. The random-walk version of the theory, originally proposed by Donley et al.,[12] avoids the requirement of the single-chain simulation step by assuming that the single chain performs a random walk in the medium-induced field. This version of the theory thus uses analytical or numerical solutions for the single-chain structure. Frischknecht and Curro used the random-walk theory by modeling their molecules as strictly Gaussian chains, where excluded volume is not enforced and thus molecules allow unrealistic backfolding. They, however, incorporated more realism into their model by modeling the interchain interactions using the Lennard-Jones form. They then compared their results with full-scale molecular dynamics simulations, where the chains were modeled as nonoverlapping bead−springs. Although the two systems were somewhat different, they found good qualitative agreement between their simulations and their theoretical results.

In this work, we use the CMS density functional theory to study properties of full, atomistically detailed (within the united atom framework) polyethylene chains of various lengths near surfaces. We also carried out a definitive test of the ability of the density functional theory to model the properties of polymers near surfaces by comparing the density functional theory results with Monte Carlo simulations of the exact same systems. One of the advantages of comparison against simulation is that the

† Part of the special issue "David Chandler Festschrift".
* To whom correspondence should be addressed.
‡ New Mexico Tech.
§ Sandia National Laboratories.
|| University of New Mexico.

10.1021/jp045597+ CCC: $30.25
Published on Web 12/21/2004

intramolecular interactions, chain architecture, torsional potentials, and molecular weights are all precisely known. A series of models are studied here with a varying range of intermolecular polymer−polymer and wall−polymer interaction strengths.

If the random-walk approximation, as used by Frischknecht and Curro, is not used, the self-consistent solution of density functional theory requires a single-chain simulation within the medium-induced potential to be performed within each step of the iteration loop. For problems involving complex systems, with approximately ∼50 iteration steps to solve a density functional equation, the computational cost of such single-chain simulations can be significant. To increase the computational efficiency of density functional theory, a few years ago Hooper et al.[13] proposed a technique to decouple the single-chain simulation step from the iterative solution by the use of an umbrella potential. In our work, we follow the methodology developed by Hooper et al. Proper use of the decoupling methodology can make the density functional solution of any complex system very efficient, though not as fast as the random-walk version[11] of the theory.

II. Density Functional Theory

The essence of the density functional theory formalism is to map the real system of interest onto an ideal system of noninteracting chains immersed in a medium-induced external field. For a known medium-induced external field, the density profile of the real system can then be estimated from simulations of a single chain in the presence of the external field. A detailed derivation of the general density functional methodology has already appeared in the literature.[13,14] Here, we merely summarize the system of equations that must be solved in our context.

Consider a polymer melt composed of chains with N spherical interaction sites, in volume V, at temperature T and chemical potential μ. The system has an inhomogeneous monomer density profile $\rho(\mathbf{r}) = \sum_\alpha \rho_\alpha(\mathbf{r})$, where $\rho_\alpha(\mathbf{r})$ is the density of site type α at $\mathbf{r}$. In the density functional theory formalism, the free energy of the system is constructed in a somewhat nonconventional grand canonical ensemble with T, V, $\rho(\mathbf{r})$, and ψ as independent variables. Here, $\psi = \mu - U_\alpha(\mathbf{r})$; $U_\alpha(\mathbf{r})$ represents an external field acting on each site of type α. Note that in a conventional grand canonical ensemble $\rho(\mathbf{r})$ is not an independent variable. An excess Helmholtz free energy is then defined above an ideal reference system, and the excess free energy of the system is constructed as a Taylor series expansion about the homogeneous liquid state, truncated after the second order. The grand potential is then related to the excess free energy with a Legendre transform. A functional minimization of the grand potential free energy with respect to the density fields provides the required expression for the medium-induced external field, which, along with the definition of the ideal system, constitutes the set of density functional equations.

The ideal system we use is a collection of noninteracting chains experiencing the exact same intramolecular interactions as the real system. The ideal system can be defined according to

$$\rho_\beta(\mathbf{r}) = \int \dots \int \exp[\sum_\alpha \psi_\alpha^{\mathrm{id}}(\mathbf{r}_\alpha)] S(\mathbf{r}_1,\dots,\mathbf{r}_N) \prod_{\alpha\neq\beta} \mathrm{d}\mathbf{r}_\alpha \quad (1)$$

where $\rho_\beta(\mathbf{r})$ is the density of the βth site in the polymer chain, the sums and products are over the N sites of the chain, and S is the N-body correlation function for a molecule of N sites. The function S restores the exact intramolecular interactions between all sites of an individual chain in the real system. $\psi_\alpha^{\mathrm{id}}(\mathbf{r}_\alpha) = \mu^{\mathrm{id}} - U_\alpha^{\mathrm{id}}(\mathbf{r}_\alpha)$, where $U_\alpha^{\mathrm{id}}(\mathbf{r}_\alpha)$ is the medium-induced external field (plus the wall potential in our case) on the αth site of the ideal chain molecule.

Derivation of the density functional equation with the above ideal system leads to the following expression for the ideal external field:

$$\beta U_\alpha^{\mathrm{id}}(\mathbf{r}) = \beta U_\alpha(\mathbf{r}) - \sum_\beta \int_V \mathrm{d}\mathbf{r}' c_{\alpha\beta}(\mathbf{r}-\mathbf{r}')\rho_\beta(\mathbf{r}') + \text{constant} \quad (2)$$

where $\beta = 1/k_\mathrm{B}T$ with k_B being the Boltzmann constant, $U_\alpha(\mathbf{r})$ is the external field due to the presence of the surface, and $c_{\alpha\beta}(\mathbf{r}-\mathbf{r}')$ is the direct correlation function between the αth and the βth site in the bulk polymer fluid.

The density profile for the inhomogeneous system is obtained by performing a single-chain (ideal system) simulation in the effective (ideal) external field. Since both density and external field are coupled through eq 2, a self-consistent solution is required. We use a simple Picard iteration scheme to obtain such a solution.

A. Decoupling of the Single-Chain Simulation Step. Self-consistent solution of eq 2 with performing a single-chain simulation at every step of the iterative loop has a few disadvantages. First, the number of iterations required to self-consistently solve the density functional equations for the polymer-near-surfaces problem is of the order of ∼50. Consequently the computational time required can be large. Second, the high computational demand of performing a single-chain simulation in each step forces one to reduce the number of simulation steps performed in each iteration loop, causing excessive noise in the simulation results. To increase the computational efficiency of density functional equations, Hooper et al.[13] proposed decoupling of the simulation step by using an umbrella potential. The single-chain simulation under an external umbrella field is performed prior to starting the self-consistent simulation loop, and chain configurations at a certain interval are saved. The density distribution, for any given medium-induced external potential, is then obtained from the weighted average:

$$\rho_\alpha(\mathbf{r}) = \left\langle \delta(|\mathbf{r}-\mathbf{r}_\alpha|) \exp(-\beta \sum_{\beta=1}^{N} [U_\alpha^{\mathrm{id}}(\mathbf{r}_\beta) - U_\mathrm{U}(\mathbf{r}_\beta)]) \right\rangle \quad (3)$$

where $U_\mathrm{U}(\mathbf{r}_\beta)$ is the umbrella potential for the βth site.

Hooper et al.[13] suggested that only one single-chain simulation with an appropriate umbrella potential would be required to obtain a complete self-consistent solution of eq 2. However, this is only true when the selected umbrella potential and the number of simulation steps would allow for the chain molecule to explore the entire phase space available with significant frequency. Since the best choice of umbrella potential or the minimum number of simulation steps required for any given problem is not known a priori, we propose the following: We first choose an arbitrary umbrella potential and obtain the iterative density functional theory solution. After self-consistency is achieved between the density profile and the medium-induced potential from using the configurations from the umbrella potential, we perform another simulation using the final potential to verify our results. If there are discrepancies between the density profiles, we restart the self-consistency loop with the new set of configurations and the potential from the last loop as our umbrella potential. Good, consistent results are usually obtained within three loops of simulation. Following

Hooper et al.,[13] we use a starting umbrella potential of the form

$$\beta U_U(z) = a\left(\frac{z - z_{center}}{z_{center}}\right)^4 \quad (4)$$

where a is an arbitrary constant that we took in the range -0.3 to -0.6, and z_{center} is halfway between the walls.

B. Direct Correlation Functions. The direct correlation functions of the bulk polymer system are required as input to the density functional theory. The direct correlation functions are obtained using the polymer reference interaction site model[15] (PRISM) theory with the atomic Percus−Yevick (PY) closure. PRISM theory is an extension to polymers of the reference interaction site model or RISM theory of Chandler and Andersen[16] for small-molecule liquids. The atomic PY relation is most successful in describing the packing structure in simple hard-core liquids. However, it does not work well when attractive tail interactions are present. We make use of the fact that for dense polymer liquids, the structure is primarily determined by the repulsive part of the potential. Consequently, for our model polyethylene molecules where intermolecular interactions are of the LJ form, we use PRISM to obtain the correlations for the repulsive part of the interactions and use a perturbation scheme following the random-phase approximation[17] (RPA) to treat the attractive tail. Molecular closures[15] and other closures[18] that include attractions have also been used with PRISM theory but are beyond the scope of the present study.

With the RPA approximation, the direct correlation function between site types α and β is

$$c_{\alpha\beta}(r) = c_{\alpha\beta}^{rep}(r) - \beta V_{\alpha\beta}^{att}(r) \quad (5)$$

where $c^{rep}(r)$ is the direct correlation function for repulsive interactions calculated from PRISM, and $V^{att}(r)$ is the attractive part of the nonbonded potential. Nath et al. previously attempted use of an RPA tail correction to the direct correlation function in the context of density functional theory in their study of symmetric block copolymers.[19,20] They found their theoretical predictions of the order−disorder phase transition to follow the same scaling as predicted from other theories. Frischknecht and Curro,[11] in their work on polymers near surfaces with the random-walk density functional theory, also used the RPA approach to treat attractions.

PRISM theory requires the intramolecular pair correlation function of the chain molecules as an input. Traditionally, an isolated chain molecule would be simulated to obtain the intramolecular correlation functions. However, the intramolecular correlation function of an isolated molecule is very different than that of a molecule in a dense liquid. To improve on the PRISM results, recently a self-consistent version of the theory has been proposed.[15] In the self-consistent PRISM theory, the intramolecular structure is obtained by simulating the isolated chain in the presence of a solvation potential which depends on the intermolecular packing of the liquid. The PRISM equation for the intermolecular correlations is solved using the determined intramolecular correlations, and then the cycle is repeated to convergence. This is carried out using reweighting techniques so that the simulation does not have to be repeated for each iteration. We use the self-consistent PRISM to calculate the direct correlation functions in this study.

Unfortunately, even with the self-consistent version of the theory, PRISM overestimates the compressibility of the liquid. Curro et al.[21] conducted a self-consistent PRISM study of polyethylene-like molecules with soft repulsive potential and found that the compressibility obtained from the theory is about 2−3 times higher than that obtained from molecular dynamics simulations. In terms of the direct correlation function, the range of the function obtained from PRISM is exactly the same as the range of the intermolecular potential due to the inherent approximation built into the PY relation. The direct correlation functions predicted from molecular dynamics simulations were longer ranged compared to those obtained from the theory. Curro et al.,[21] in their study, empirically added an attractive tail to $C(r)$ obtained from PRISM theory to improve the long-range behavior of the direct correlation function. The tail was chosen to match the predicted zero wave vector structure factor from simulation. We did not attempt such a correction in this work, as that would require us to perform a full-scale simulation of the bulk liquids. Instead, we follow the approach used by Frischknecht and Curro[11] and compensate for the long-range correlation by adding a multiplicative factor to the PRISM-predicted function.

$$c_{\alpha\beta}(r) = K_1 c_{\alpha\beta}^{PRISM}(r) \quad (6)$$

For attractive systems, we attempt the correction in two different ways. In the first approach, we correct the repulsive PRISM-predicted function following eq 6 to obtain

$$c_{\alpha\beta}(r) = K_1 c_{\alpha\beta}^{rep,PRISM}(r) - \beta V_{\alpha\beta}^{att}(r) \quad (7)$$

In the second approach, we emphasize the fact that the PRISM-predicted direct correlation function for the repulsive system at short length scales agrees well with that predicted from simulations. The discrepancy between the two exists on long length scales. Hence we attempt to compensate for that by adding a multiplicative factor (<1.0) to the attractive RPA part of the correlation function.

$$c_{\alpha\beta}(r) = c_{\alpha\beta}^{rep,PRISM}(r) - K_2 \beta V_{\alpha\beta}^{att}(r) \quad (8)$$

III. Model

We model our polyethylene chains following the NERD model of Nath et al.[22] NERD is a united atom potential model where hydrogen atoms are not represented explicitly, and thus methyl (CH_3) and methylene (CH_2) groups are treated as single interaction sites. For simplicity, in our work we model alkane chains as consisting of CH_2 sites only, including the end sites. This is chemically unphysical; however, having CH_2 rather than CH_3 terminal sites should not appreciably affect the packing. Note that this is by no means a limitation of the theory as it is fully capable of treating more than one type of interaction site. Unlike the NERD model, we use a fixed bond length (1.54 Å) between the overlapping CH_2 sites. For bending and torsion, we use the same potentials as used in NERD. A harmonic potential is used to represent the bending potential,

$$V_b(\theta) = K_b(\theta - \theta_b)^2 \quad (9)$$

where K_b is the potential constant and θ_b is the equilibrium angle. A cosine series is used to represent the torsional potential,

$$V_t(\varphi) = a_0 + a_1(1 + \cos\varphi) + a_2(1 - \cos 2\varphi) + a_3(1 + \cos 3\varphi) \quad (10)$$

And finally, the nonbonded interactions and interactions between atoms separated by more than three bonds in the same molecule are represented by the 12−6 Lennard-Jones potential

$$V(r) = 4\epsilon\left[\left(\frac{\sigma}{r}\right)^{12} - \left(\frac{\sigma}{r}\right)^{6}\right] \quad (11)$$

Parameters associated with the angular potentials and nonbonded interactions are given in Table 1.

As mentioned earlier, PRISM theory is solved with the repulsive part of the LJ interactions. To this end, we decompose the full LJ interaction to a repulsive part $V^{rep}(r)$ following Weeks, Chandler, and Andersen[23]

$$V^{rep}(r) = 4\epsilon\left[\left(\frac{\sigma}{r}\right)^{12} - \left(\frac{\sigma}{r}\right)^{6}\right] + \epsilon \qquad r \le 2^{1/6}\sigma$$
$$= 0 \qquad r > 2^{1/6}\sigma \quad (12a)$$

and an attractive or perturbative part $V^{att}(r)$,

$$V^{att}(r) = -\epsilon \qquad r \le 2^{1/6}\sigma$$
$$= 4\epsilon\left[\left(\frac{\sigma}{r}\right)^{12} - \left(\frac{\sigma}{r}\right)^{6}\right] \qquad r > 2^{1/6}\sigma \quad (12b)$$

However, when applying the RPA correction to the PRISM-calculated direct correlation function we recognize the fact that addition of ϵ to the repulsive potential at very short distances of r does not have any effect on its strength. Thus, making an attractive correction at those distances actually is not required. We apply our RPA correction to the direct correlation function at distances $r \ge 0.8 \times 2^{1/6}\sigma$ only. While working with attractive systems, we also truncate the attractive tail at a distance of 10 Å and shift the whole curve such that the potential is zero at the cutoff.

We model our system as polyethylene liquid confined in a slit pore. We set the distance between two walls to be 50 Å, in the z direction, throughout this paper. The system is considered infinite in both the x and the y directions. Both the walls are identical and interact uniformly with the polymer fluid. We considered two types of wall polymer interactions. The first is a hard wall,

$$V_{wall-polymer}(z) = \infty \qquad z \le 0$$
$$= 0 \qquad z > 0 \quad (13)$$

The second is a modified Lennard-Jones interaction of the form appropriate for flat surfaces,[24]

$$V_{wall-polymer}(z) = \infty \qquad z \le 0$$
$$= \left(\frac{2\pi\epsilon_{wp}\rho_w\sigma_{wp}^3}{3}\right)\left[\frac{2}{15}\left(\frac{\sigma_{wp}}{r+\xi\sigma_{wp}}\right)^9 - \left(\frac{\sigma_{wp}}{r+\xi\sigma_{wp}}\right)^3\right] \qquad z > 0 \quad (14)$$

where ρ_w is the density of the wall and $\xi = (2/15)^{1/6}$.

We considered two different sizes of alkanes in this study, namely, C_{12} and C_{24}. In each case, we picked the systems to have the experimental densities at a given temperature and 1 bar.[25−27] Complete details of system temperatures and densities studied are given in Table 2.

IV. Monte Carlo Simulations

Three types of simulations were carried out in this work. The first is the simulation of a single chain in the solvation potential provided by the self-consistent PRISM theory. The second is the simulation of a single chain in the presence of the medium-induced and/or umbrella potentials during DFT solution. The third type includes many-chain simulations of alkane molecules with repulsive and attractive interactions, confined between the repulsive and attractive surfaces. These many-chain simulations are then used to compare with the DFT calculations.

TABLE 1: Angular and Lennard-Jones Parameters for All the Polyethylene Models

K_b (bending)	90.75	kcal/(mol rad^2)
θ_b	114.0	
a_0 (torsion)	0.0	kcal/mol
a_1	0.70507	
a_2	−0.1354	
a_3	1.5714	
ϵ (nonbonded)	0.09095	kcal/mol
σ	3.93	Å

TABLE 2: Experimental Densities of All Polyethylene Models at 1 bar

molecule	temperature (K)	density (sites/Å^3)
C_{12}	525.0	0.0241
C_{12}	375.0	0.02933
C_{24}	405.0	0.03097

In all the Monte Carlo simulations, we used three different types of moves: pivot bending, pivot torsion, and translation. For the bending moves, a random angle-triplet was picked and one arm of the triplet was rotated by a random angle (usually between ±30°) around the axis perpendicular to the triplet plane. For the torsion moves, a dihedral quadruplet was chosen at random and the shorter of the two arms was rotated around the center axis by a random angle between ±180°. For the translation moves, the complete molecule was translated in a random direction (usually between ±1 Å). Translation moves do not have any significance for simulations during PRISM solution and thus were not used. For more details on the implementation of these moves and simulations during self-consistent PRISM solution, readers are referred to an earlier publication.[28]

The simulations of a single chain (ideal chain) in the medium-induced potential and/or umbrella potential for the DFT calculations were carried out between two parallel, flat walls. A periodic boundary condition was implemented in the x and the y directions. Due to the presence of the walls, a periodic boundary does not apply in the z direction. When performing simulations with an umbrella potential, configurations of the molecule were saved in a file at an interval of 50 steps. Configurations are later read from the file when performing the weighted average in eq 3 in obtaining the density profiles for a particular medium-induced potential. Symmetry conditions were used to average the density profiles around the symmetry line between the two walls. The density at the middle between the two walls is set based on conservation of mass for the polymer solution between the two walls.

Although saving configurations in a file and reading them when necessary adds additional computational time, it is negligible compared to that in performing a complete simulation at every step of the DFT solution. By not saving the configurations in the memory, we also gain a huge advantage in terms of not increasing the computer memory requirement during the solution. When solving the density functional equations using a Picard iteration scheme, it is necessary to mix the "old" and "new" density profiles at every step of the iteration procedure. We mix 5% of the new density profile at every step of the iteration.

The length of our single-chain simulations, used during solution of the density functional equations, was about 1×10^7 Monte Carlo steps. Each Monte Carlo step consisted of one

pivot bending, one pivot torsion, and one translation move. The percentage of acceptance of MC moves during these simulations was about 30−40% for pivot bending, about 25−35% for pivot rotation moves, and about 70−80% for translation moves. The time required for completing a DFT solution was about 30−40 min for C_{12} molecules and about 2 h for the C_{24} molecules on a 1.4 GHz Intel Pentium Centrino Mobile processor.

Full Monte Carlo simulations were conducted in the *NVT* ensemble. Our simulations were conducted on samples of 80 molecules for C_{12} and 60 molecules for C_{24} systems, using a conventional Metropolis sampling scheme. The simulation box was confined in the *z* direction by two walls, and periodic boundary conditions were applied in the *x* and the *y* directions. The typical length of simulations was in the order of 3×10^6 steps. Multichain simulations of confined systems are computationally demanding and were performed only on a few select systems. The percentage of acceptance of MC moves during these simulations was about 15−25% for both pivot bending and pivot rotation moves and about 10−15% for translation moves for the C_{12} molecules. For the C_{24} molecules, the acceptance rates were only about 15−20% for pivot bending, about 6−8% for pivot rotation moves, and about 5−6% for translation moves. It became apparent that full-scale simulation of longer chain molecules at comparable densities would not be possible with our current implementation and would require more efficient and sophisticated Monte Carlo techniques.[29]

V. Results

A. Repulsive Systems. We begin by comparing the results from our density functional theory to the full-scale Monte Carlo simulations for the repulsive systems. In this work, for a repulsive system, the polymer is modeled as nonbonded sites interacting through a LJ potential that is truncated and shifted at the potential minimum as shown in eq 12a, and the wall is modeled as hard wall as shown in eq 13. Previously, Hooper et al.[30] compared simulation results to DFT results solved with PRISM-PY-predicted direct correlation functions for hard chains near hard surfaces. For their bead−spring model polymer systems, they found that DFT predictions are in quite good agreement with simulation predictions. Density at the wall contact predicted from the theory was slightly lower than the simulation results, and the theory also predicted slightly less structure compared to the simulation. Since the compressibility predicted from PRISM-PY for such systems is always too high ($C(r)$ values are always low), one should expect that the density profile predicted with PRISM-PY should show less structure. Hooper et al.[29] found better than expected results due to a fortuitous cancellation of errors as the DFT field described in eq 2 is too strong but is compensated for by the lower values of $C(r)$.

Based on the findings of Curro et al.[21] that PRISM-PY theory is more accurate for tangent site models compared to a realistically detailed polymer model used in the current work, we expect that our comparison of DFT-PRISM-PY results should also show less structure compared to simulations. We see this expected behavior in all three systems displayed in Figures 1−3. The DFT prediction of density near the wall is considerably lower than those predicted from simulations. One should exercise care here in judging the predictive ability of the current version of density functional theory because the major cause of this discrepancy is rooted in the PRISM-PY predictions. The opposite trend was observed when Frischknecht and Curro[11] compared their random-walk DFT with the simulation results for bead−spring polymers near soft−repulsive walls.

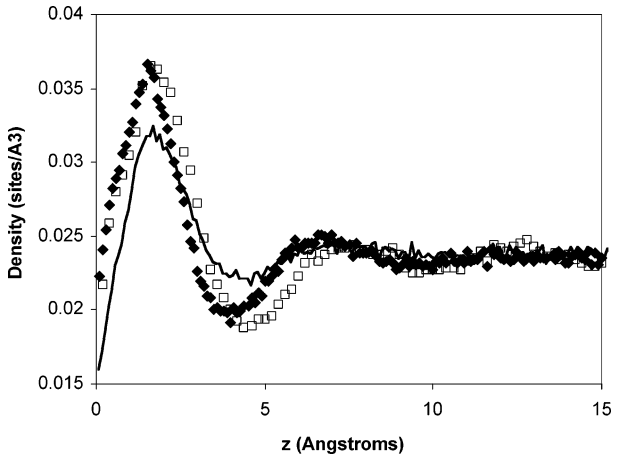

Figure 1. Comparison of density profiles from density functional theory and Monte Carlo simulations of C_{12} at $T = 525$ K. Polymer nonbonded interactions are modeled as repulsive LJ, and the wall interaction is modeled as a hard wall. The meanings of the symbols and lines are as follows: line (density functional theory with PRISM input), filled symbols (density functional theory with $c(r) = 1.5c^{\mathrm{PRISM}}(r)$ input), open symbols (simulation).

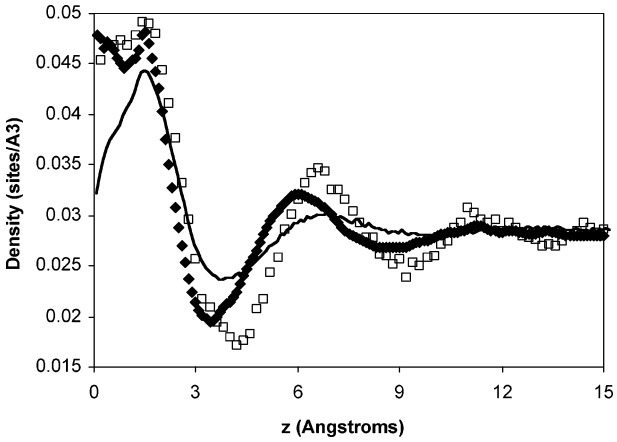

Figure 2. Comparison of density profiles from density functional theory and Monte Carlo simulations of C_{12} at $T = 375$ K. Polymer nonbonded interactions are modeled as repulsive LJ, and the wall interaction is modeled as a hard wall. The meanings of the symbols and lines are as follows: line (density functional theory with PRISM input), filled symbols (density functional theory with $c(r) = 1.4c^{\mathrm{PRISM}}(r)$ input), open symbols (simulation).

They found that their DFT-PRISM-PY results actually showed more structure compared to the simulation results. We believe that the cause of this unexpected trend was due to the fact that their DFT chains were completely Gaussian, whereas their MD simulations enforced excluded volume interactions.

To improve the accuracy of DFT predictions, one approach is to correct the PRISM-PY direct correlation functions before applying them to the DFT calculation. One could, in principle, obtain the correct isothermal compressibility of the system, either from known equations-of-state or from performing a full-scale simulation of the bulk system and modifying $C(r)$ using thermodynamic relations. In fact, bypassing the PRISM calculations, direct correlation functions obtained from a full-scale simulation of the bulk system could also be used as input to the DFT calculations. However, use of the exact $C(r)$ would likely produce too much structure in the density profile since it is known that the field in eq 2 is too strong. In this work, we focus on using PRISM-PY theory for the direct correlation functions since in general the equation-of-state is not available, and we seek the density profile without resorting to full many-

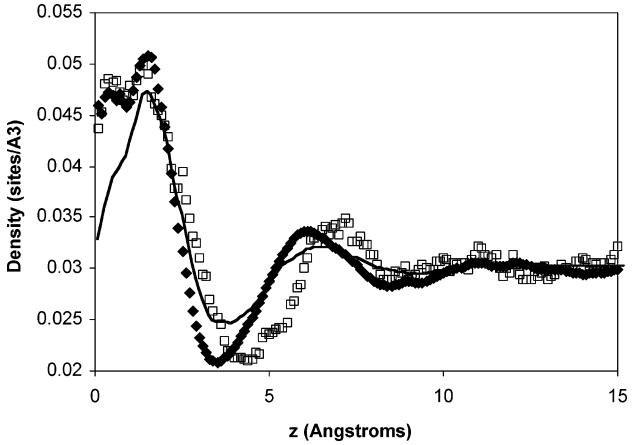

Figure 3. Comparison of density profiles from density functional theory and Monte Carlo simulations of C_{24} at $T = 405$ K. Polymer nonbonded interactions are modeled as repulsive LJ, and the wall interaction is modeled as a hard wall. The meanings of the symbols and lines are as follows: line (density functional theory with PRISM input), filled symbols (density functional theory with $c(r) = 1.4c^{\mathrm{PRISM}}(r)$ input), open symbols (simulation).

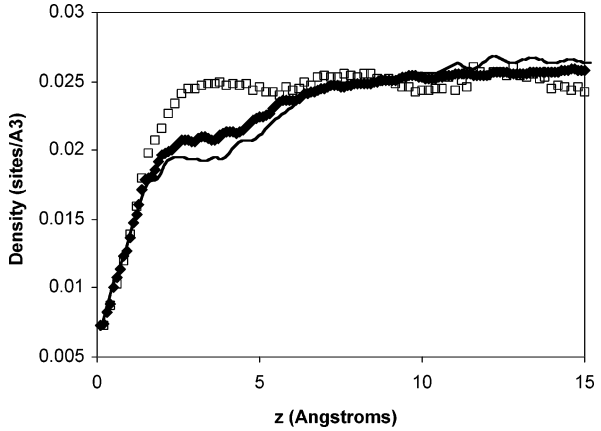

Figure 4. Comparison of density profiles from density functional theory and Monte Carlo simulations of C_{12} at $T = 525$ K. Polymer nonbonded interactions are modeled as LJ, and the wall interaction is modeled as a hard wall. The meanings of the symbols and lines are as follows: line (DFT with eq 7, $K_1 = 1.5$), filled symbols (DFT with eq 8, $K_2 = 0.6$), open symbols (simulation).

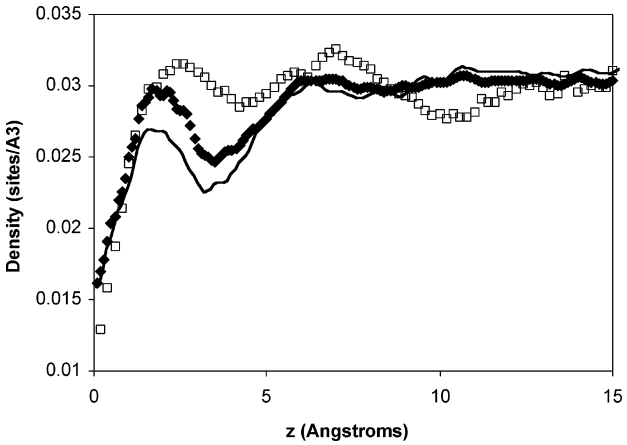

Figure 5. Comparison of density profiles from density functional theory and Monte Carlo simulations of C_{12} at $T = 375$ K. Polymer nonbonded interactions are modeled as LJ, and the wall interaction is modeled as a hard wall. The meanings of the symbols and lines are as follows: line (DFT with eq 7, $K_1 = 1.4$), filled symbols (DFT with eq 8, $K_2 = 0.6$), open symbols (simulation).

chain simulations. We thus use eq 6 to correct PRISM-PY results, with a somewhat ad hoc approach to set the constant K_1. We set the multiplicative factor in eq 6 such that the DFT-calculated density profile predicts the wall contact density with reasonable accuracy. Density profiles predicted from the corrected PRISM-PY direct correlation functions are also shown in Figures 1−3. For the C_{12} system at 525 K (Figure 1), a value of $K_1 = 1.5$ was used, and for the other two systems $K_1 = 1.4$ was used. In all three cases, DFT-predicted density profiles are now in reasonable agreement with the simulation results. DFT results at lower density and higher temperature are reproduced slightly better than the higher density, lower temperature systems. For high-density systems, especially for C_{12} at 375 K, simulations produce a long-range density oscillation that is absent in the DFT results. The lack of density oscillations at longer range may be related to the fact that, even with the corrections in eq 6, the direct correlation function used here is short ranged compared to what one would obtain from a bulk, full-scale simulation.

B. Attractive Polymers, Hard Surfaces. As our goal is to study more realistically detailed systems, we turn on the attractions in our systems slowly. First, we performed full many-chain simulations and DFT calculations on systems where the wall interactions are still modeled as hard wall, but the polymer interactions are modeled with full LJ. Note that it is possible for such systems to produce dewetting. One should also be careful in dealing with attractive polymer systems, not to be dealing with state conditions where the polymer may exhibit vapor−liquid equilibrium. For our alkane systems, we picked the system densities based on the experimentally predicted liquid region. The NERD force field used in this study is very accurate in predicting the vapor−liquid equilibrium region. Also, by making the simplification to model the end groups as CH_2 groups in this work our systems are pushed further into the liquid region.

As described earlier, we truncate and shift the LJ potential at a distance of 10 Å in modeling attractive nonbonded interactions in the polymer. In modeling the long-range interactions for our PRISM-PY predictions through eq 7, we use the same values of K_1 as used in the earlier section. Figures 4 and 5 show the density profiles predicted for the two temperatures for C_{12}. Without any further adjustments to the direct correlation function, the theory predicts density profiles near the surface surprisingly well. However, the theory underestimates the magnitude of the first peak in the profile.

We now attempt to model the long-range interactions in the PRISM-PY theory using eq 8. Once again, we use the ad hoc procedure of adjusting the density near the wall contact to obtain a value of K_2. By adjusting for the system at 525 K, we obtain a value of $K_2 = 0.6$. We use the same value for the higher density, lower temperature system. With this approach to adjusting the direct correlation function for the attractive system, the quality of the results near the wall contact remain unchanged, but improvements are observed around the first peak (Figures 4 and 5). Nevertheless, density profiles near the first peak are still underpredicted from the theory, in comparison to simulation results.

C. Attractive Polymers, Attractive Surfaces. We now turn on the surface attractions using eq 14 to study more realistic systems having both surface/polymer and polymer/polymer attractive forces. We used a value of $\rho_w\sigma_{wp}^3 = 2.0$ and $\sigma_{wp} = \sigma_{\mathrm{methylene}}$ in both our full many-chain simulations and DFT calculations. These choices give a wall density of 0.0337 sites/Å^3, which is only slightly higher than the polymer densities

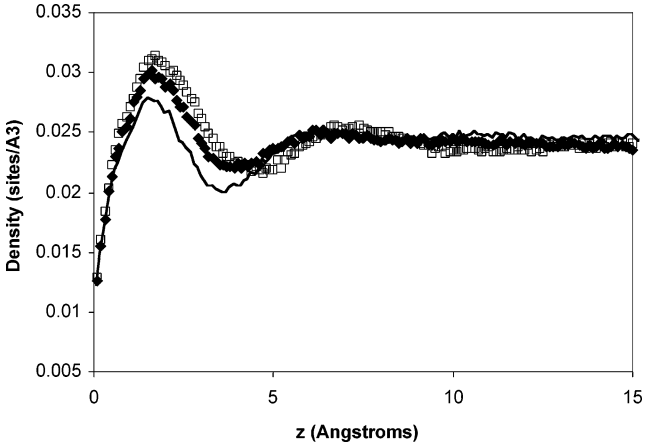

Figure 6. Comparison of density profiles from density functional theory and Monte Carlo simulations of C_{12} at $T = 525$ K. Attractive polymer, attractive surfaces system with $\epsilon_{wp} = \epsilon$. The meanings of the symbols and lines are as follows: line (DFT with eq 7, $K_1 = 1.5$), filled symbols (DFT with eq 8, $K_2 = 0.6$), open symbols (simulation).

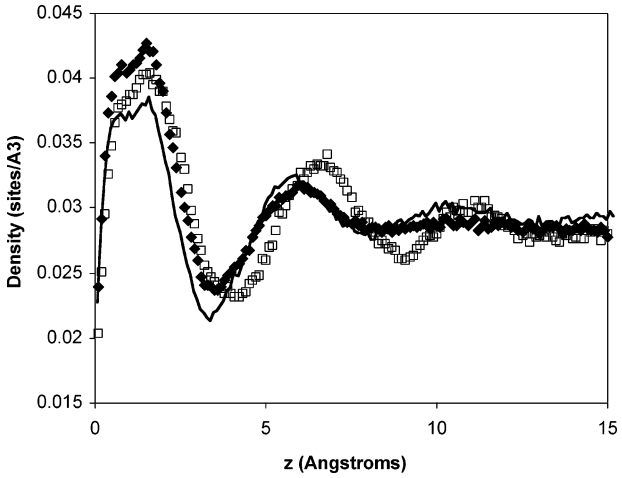

Figure 7. Comparison of density profiles from density functional theory and Monte Carlo simulations of C_{12} at $T = 375$ K. Attractive polymer, attractive surfaces system with $\epsilon_{wp} = \epsilon$. The meanings of the symbols and lines are as follows: line (DFT with eq 7, $K_1 = 1.4$), filled symbols (DFT with eq 8, $K_2 = 0.6$), open symbols (simulation).

studied. We first consider systems where the wall−polymer interaction strength ϵ_{wp} is the same as the polymer−polymer interaction strength ϵ. We continue to use eqs 7 and 8 for direct correlation functions with K_1 and K_2 values obtained earlier without making any further empirical adjustments. With the addition of the attractive wall for the C_{12} at 525 K system, the DFT with eq 8 approach for long-range interactions shows major improvements over the attractive polymer/hard surfaces system. As shown in Figure 6, the DFT prediction for this system is in quantitative agreement with the simulation results. Results for the C_{12} system at 375 K (Figure 7) and the C_{24} system at 405 K (Figure 8) are also in reasonable agreement with the simulation results. For these systems, the DFT prediction of the wall contact density is slightly higher but the magnitude and position of the first density peak are well predicted. In all these cases, DFT, using the eq 7 approach, is slightly inferior to its eq 8 counterpart.

To understand the effect of wall−polymer interaction strength on the density functional theory predictions, we consider systems with varying wall−polymer interaction strength for the C_{12} system at 375 K. Figure 9 displays the density profile of a system where the wall−polymer interaction strength is twice

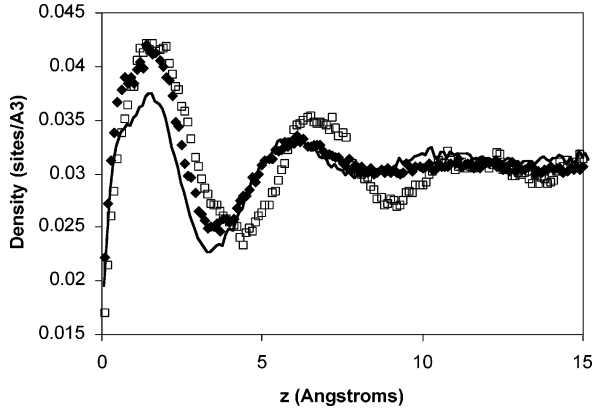

Figure 8. Comparison of density profiles from density functional theory and Monte Carlo simulations of C_{24} at $T = 405$ K. Attractive polymer, attractive surfaces system with $\epsilon_{wp} = \epsilon$. The meanings of the symbols and lines are as follows: line (DFT with eq 7, $K_1 = 1.4$), filled symbols (DFT with eq 8, $K_2 = 0.6$), open symbols (simulation).

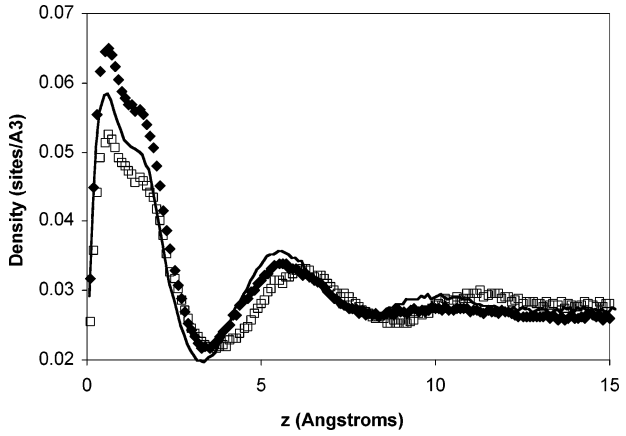

Figure 9. Comparison of density profiles from density functional theory and Monte Carlo simulations of C_{12} at $T = 375$ K. Attractive polymer, attractive surfaces system with $\epsilon_{wp} = 2\epsilon$. The meanings of the symbols and lines are as follows: line (DFT with eq 7, $K_1 = 1.4$), filled symbols (DFT with eq 8, $K_2 = 0.6$), open symbols (simulation).

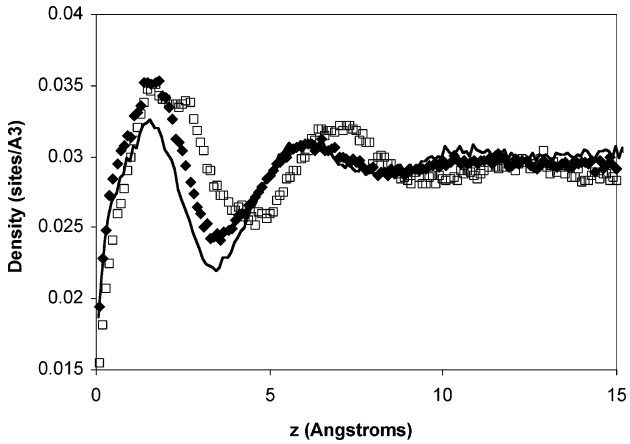

Figure 10. Comparison of density profiles from density functional theory and Monte Carlo simulations of C_{12} at $T = 375$ K. Attractive polymer, attractive surfaces system with $\epsilon_{wp} = 0.5\epsilon$. The meanings of the symbols and lines are as follows: line (DFT with eq 7, $K_1 = 1.4$), filled symbols (DFT with eq 8, $K_2 = 0.6$), open symbols (simulation).

as strong as the polymer−polymer interaction strength, and Figure 10 displays the density profile of a system where the wall−polymer interaction strength is half of the polymer−polymer interaction strength. We continue to use K_1 and K_2 values as before. DFT results for the system with $\epsilon_{wp} = 0.5\epsilon$

(Figure 10) are comparable to those for the system with $\epsilon_{wp} = \epsilon$ (Figure 7). With the eq 8 approach, the DFT prediction of the wall contact density is slightly higher compared to that from Monte Carlo predictions, but the magnitude of the first density peak is well predicted. However, for the weaker wall−polymer interaction strength system, the width of the first peak predicted from DFT is narrower compared to that predicted from Monte Carlo simulation. As before, results using the eq 7 approach are slightly inferior to those using the eq 8 approach.

When we increase the wall−polymer interaction strength to twice that of the polymer−polymer interaction strength, we observe that DFT tends to overestimate the magnitude of the first peak, along with the contact density as before. In this case, however, the rest of the density profile is well predicted. Unlike our previous observations, here predictions using eq 7 agree with the Monte Carlo simulations better than the results from eq 8. It is quite apparent from these figures that for systems with attractive polymer−polymer interactions, DFT handles the cases well when wall−polymer interactions are comparable to the polymer−polymer interactions. DFT results start to deviate more from the Monte Carlo simulation results as the wall−polymer interaction strength is increased or decreased.

VI. Conclusions

Density profiles for realistically detailed polyethylene melts near a surface have been calculated using the structure-based density functional theory of Chandler, McCoy, and Singer and compared to Monte Carlo simulations. The primary input to the density functional theory, the direct correlation function, was obtained using the self-consistent PRISM theory with the PY closure for the repulsive potentials and then correcting for the attractive LJ tail via use of the random-phase approximation.

For purely repulsive systems, we expect a cancellation of errors since the large compressibility from PRISM tends to be canceled by the field in eq 2 that is too strong. This cancellation is not complete for our atomistic polyethylene calculations since the uncorrected density profiles show less structure compared to Monte Carlo simulation. When the direct correlation functions are empirically corrected by using a multiplication factor, the DFT results improve significantly to provide reasonable agreement with simulation results.

To include the effect of polymer attractions on the density profile, we also made multiplicative corrections to the PRISM-PY-generated direct correlation function while adding the RPA tail correction. We tried two different approaches in obtaining the corrected direct correlation functions for the attractive systems. In the first approach, the PRISM-PY-predicted correlation functions for the repulsive system were first corrected and then the full RPA attractions were added. In the second approach, the PRISM-PY-predicted correlation functions for the repulsive system were kept as is, and a multiplicative reduction was done to the RPA attractions. The latter approach implicitly takes care of the fact that PRISM-PY produces direct correlation functions of the repulsive systems that are too short ranged. In our DFT calculations, we found that scaling the RPA attractions (rather than the repulsive part of $C(r)$) tended to yield density profiles in better agreement with simulations for attractive systems.

Unlike in a bulk liquid, a site near the surface of a nonuniform system feels nonisotropic forces on the average. Whether this results in an increase or a decrease of the surface density depends on a delicate balance between the surface/polymer and the polymer/polymer attractions. The challenge for DFT is to accurately predict this balance of attractions. Not surprisingly, we found that our DFT/PRISM approach was most accurate when the wall and polymer attractions were of comparable magnitude. The DFT/PRISM theory presented here predicts surprisingly accurate density profiles in view of its simplicity. Further improvements will require more accurate direct correlation functions designed to reproduce the equation-of-state of the bulk polymer liquid. At the same time, a more accurate form of the field needs to be constructed in order to accurately account for the balance of surface and polymer attractions. Efforts along this line are currently underway.

As we have demonstrated in this study, a DFT theory capable of describing atomistic models of polymers is possible without the investment of large computational resources. Even though a single-chain simulation is required, use of the reweighting techniques of Hooper et al.[13] allows the simulation to be decoupled from the self-consistent part of the problem. As a consequence, the computer requirements using our DFT approach are orders of magnitude smaller than for the corresponding many-chain simulation. This makes it possible to study many important problems related to polymers near surfaces at the atomistic level. Using this approach, one can account for the effect of local chain architecture on the packing of macromolecules near surfaces.

Acknowledgment. Sandia is a multiprogram laboratory operated by Sandia Corporation, a Lockheed Martin Company, for the United States Department of Energy's National Nuclear Security Administration under Contract DE-AC04-94AL85000. The authors thank A. Frischknecht for helpful discussions.

References and Notes

(1) Chandler, D.; McCoy, J. D.; Singer, S. J. *J. Chem. Phys.* **1986**, *85*, 5971.

(2) Chandler, D.; McCoy, J. D.; Singer, S. J. *J. Chem. Phys.* **1986**, *85*, 5977.

(3) McCoy, J. D.; Singer, S. J.; Chandler, D. *J. Chem. Phys.* **1987**, *87*, 4853.

(4) Sen, S.; Cohen, J. M.; McCoy, J. D.; Curro, J. G. *J. Chem. Phys.* **1994**, *101*, 3205.

(5) Sen, S.; McCoy, J. D.; Nath, S. K.; Donley, J. P.; Curro, J. G. *J. Chem. Phys.* **1994**, *102*, 3431.

(6) Flory, P. J. *Statistical Mechanics of Chain Molecules*; Wiley: New York, 1969.

(7) Woodward, C. E.; Yethiraj, A. *J. Chem. Phys.* **1994**, *100*, 3181. Yethiraj, A.; Woodward, C. E. *J. Chem. Phys.* **1995**, *102*, 5499.

(8) Patra, C. N.; Yethiraj, A. *J. Chem. Phys.* **2003**, *118*, 4702.

(9) Forsman, J.; Woodward, C. E.; Freasier, B. C. *J. Chem. Phys.* **2002**, *116*, 4715.

(10) Christopher, P. S.; Oxtoby, D. W. *J. Chem. Phys.* **2003**, *119*, 10330.

(11) Frischknecht, A. L.; Curro, J. G. *J. Chem. Phys.* **2004**, *121*, 2788.

(12) Donley, J. P.; Rajasekaran, J. J.; McCoy, J. D.; Curro, J. G. *J. Chem. Phys.* **1995**, *103*, 5061.

(13) Hooper, J. B.; McCoy, J. D.; Curro, J. G. *J. Chem. Phys.* **2000**, *112*, 3090.

(14) For a review see: McCoy, J. D.; Nath, S. K. *Chemical Applications of Density Functional Theory*; Laird, B. B., Ross, R. B., Ziegler, T., Eds.; American Chemical Society: Washington, DC, 1996.

(15) For a review see: Schweizer, K. S.; Curro, J. G. *Adv. Chem. Phys.* **1997**, *98*, 1. Schweizer, K. S.; Curro, J. G. *Adv. Polym. Sci.* **1994**, *116*, 321.

(16) Chandler, D.; Andersen, H. C. *J. Chem. Phys.* **1972**, *57*, 1930. Chandler, D. In *Studies in Statistical Mechanics VIII*; Montroll, E. W., Lebowitz, J. L., Eds.; North-Holland: Amsterdam, 1982; p 274.

(17) Hansen, J. P.; McDonald, I. R. *Theory of Simple Liquids*, 2nd ed.; Academic Press: London, 1986.

(18) Livadaru, L.; Kovelenko, A. *J. Chem. Phys.* **2004**, *121*, 4449.

(19) Nath, S. K.; McCoy, J. D.; Curro, J. G.; Saunders, R. S. *J. Chem. Phys.* **1997**, *106*, 1950.

(20) McCoy, J. D.; Nath, S. K.; Curro, J. G.; Saunders, R. S. *J. Chem. Phys.* **1998**, *108*, 3023.

(21) Curro, J. G.; Webb, E. B., III; Grest, G. S.; Weinhold, J. F.; Putz, M.; McCoy, J. D. *J. Chem. Phys.* **1999**, *111*, 9073.
(22) Nath, S. K.; Escobedo, F. A.; de Pablo, J. J. *J. Phys. Chem.* **1198**, *108*, 9905.
(23) Weeks, J. D.; Chandler, D.; Andersen, H. C. *J. Chem. Phys.* **1971**, *54*, 5237.
(24) Steele, W. A. *The Interaction of Gases with Solid Surfaces*; Pergamon Press: Oxford, 1974.
(25) Olabisi, O.; Simha, R. *J. Appl. Polym. Sci.* **1997**, *21*, 149.
(26) Olabisi, O.; Simha, R. *Macromolecules* **1995**, *8*, 211.
(27) Nath, S. K.; McCoy, J. D.; Curro, J. G. *Macromolecules* **1995**, *28*, 3275.
(28) Putz, M.; Curro, J. G.; Grest, G. S. *J. Chem. Phys.* **2001**, *114*, 2847.
(29) Escobedo, F. A. Ph.D. Thesis, University of Wisconsin—Madison, Madison, WI, 1998.
(30) Hooper, J. B.; Pileggi, M. T.; McCoy, J. D.; Curro, J. G.; Weinhold, J. D. *J. Chem. Phys.* **2000**, *112*, 3094.